

Supporting Information for

An unique magnesium-based 3D MOF with nanoscale cages showing temperature dependent selective gas sorption properties

Yong-Liang Huang, Yun-Nan Gong, Long Jiang, and Tong-Bu Lu^{*}

Experimental section

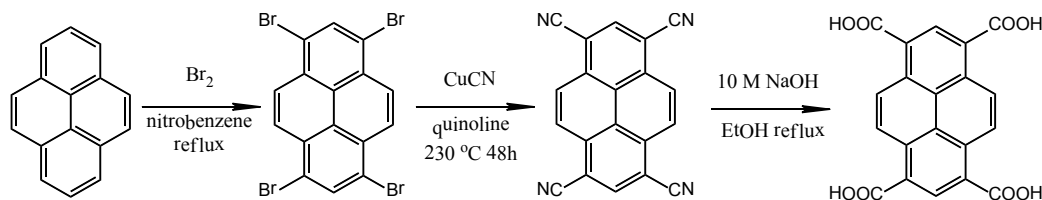
Materials and general methods.

The 1,3,6,8-Tetracyanopyrene (TCNP) was synthesized by a literature method¹, and all the other solvents and chemicals were commercially available and used without further purification. Electrospray ionization (ESI) mass spectra were performed on a Thermo Finigan LCQ DECA XP ion trap mass spectrometer in DMF. Elemental analyses were determined using an Elementar Vario EL elemental analyzer. The IR spectra were recorded in the 4000-400 cm⁻¹ region using KBr pellets and a Bruker EQUINOX spectrometer. Thermogravimetric analyses (TGA) data were collected on a Netzsch TG-209 instrument with a heating rate of 10 °C min⁻¹. The X-ray powder diffraction (XRD) measurements were recorded on a D8 ADVANCE X-ray diffractometer. The single crystal data were collected on a Xcalibur Atlas Gemini ultra diffractometer.

Synthesis of pyrene-1,3,6,8-tetracarboxylic acid (H₄PTCA).

A mixture of 1,3,6,8-Tetracyanopyrene (TCNP) (2.26 g, 7.5 mmol), aqueous

solution of NaOH (10 M, 60 mL) and ethanol (90 mL) was heated at reflux in a 250 mL round-bottom flask for 1 day. Upon cooling to room temperature, the mixture was acidified with 37 % hydrochloric acid until pH = 1. The product, H₄PTCA, was collected by filtration, washed with water and ethanol, yield: 1.84 g, 65%. Anal. Calcd for C₂₀H₁₀O₈·(H₂O)_{6.5}: C, 48.49; H, 4.68; N, 0.00. Found: C, 48.65; H, 4.33; N, 0.18. IR (KBr, cm⁻¹): 3232 (s), 3133 (s), 3099 (s), 3067 (s), 2852 (m), 1886 (w), 1733 (vs), 1656 (vs), 1562 (s), 1509 (m), 1437 (s), 1394 (m), 1365 (w), 1316 (w), 1242 (s), 1206 (s), 1185 (s), 1117 (s), 1034 (w), 944 (w), 846 (s), 746 (w), 643 (m). m/z (ESI-MS): 377 for [H₃PTCA]⁺.



Scheme S1. Synthetic route for H₄PTCA.

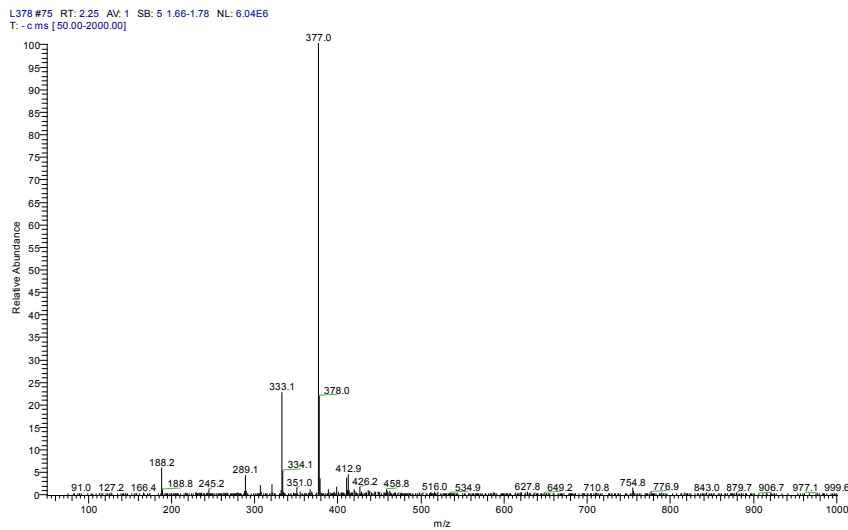


Fig. S1. ESI mass spectrum of H₄PTCA.

Synthesis of [Mg₁₆(PTCA)₈(μ₂-H₂O)₈(H₂O)₁₆(Dioxane)₈]·(H₂O)₁₃·(DMF)₂₆ (**1**).

A mixture of 0.15 mmol (30 mg) MgCl₂·6H₂O, 0.06 mmol (23 mg) H₄PTCA, and

1.2 M HCl (1 drop) was added to 8 mL of a mixture solution of DMF/dioxane/H₂O (2:1:1). After stirred for ten minutes, the solution was transferred to Teflon-lined autoclave and heated at 90 °C for 72 h. The autoclave was cooled over a period of 14 h at a rate of 5 °C·h⁻¹. Yellow block crystals of **1** were collected with a yield of 60% (based on Mg). Anal. Calcd for (C₂₇₀H₃₆₈N₂₆O₁₄₃Mg₁₆): C, 48.73; H, 5.57; N, 5.47. Found: C, 48.82; H, 5.29; N, 5.67. IR (KBr, cm⁻¹): 3398 (vs), 2960 (m), 2931 (m), 2809 (m), 2280 (w), 2076 (w), 1656 (vs), 1632 (vs), 1502 (w), 1396 (vs), 1374 (vs), 1315 (s), 1254 (m), 1179 (w), 1149 (w), 1103 (m), 1023 (m), 856 (m), 801 (s), 723 (m), 673 (s), 577(w).

Determination of the crystal structure.

Single-crystal X-ray diffraction data for **1** were collected on a Xcalibur Atlas Gemini ultra diffractometer, with Cu-K α radiation ($\lambda = 1.54178 \text{ \AA}$) at 150(2) K. The numerical absorption corrections were applied using the program of ABSCOR. The structure was solved using direct method, which yielded the positions of all non-hydrogen atoms. These were refined first isotropically and then anisotropically. All of the hydrogen atoms of the ligands were placed in calculated positions with fixed isotropic thermal parameters and included in the structure factor calculations in the final stage of full-matrix least-squares refinement. All calculations were performed using the SHELXTL system of computer programs. The unit cell volume included a large region of disordered solvent which could not be modelled as discrete atomic sites. Due to very large highly disordered solvent accessible void space in the framework, the diffraction data are relatively weak. Restraints (SADI and DFIX) were

applied for disordered Mg ions, dioxane and water molecules. SQUEEZE subroutine of the PLATON software suite was applied to remove the scattering from the highly disordered guest molecules. The resulting new HKL files were used to further refine the structures. The final formula was calculated from the SQUEEZE results combined with elemental analysis data and TGA data. The crystallographic data are summarized in Table S1, and the selected bond lengths and angles are listed in Table S2.

Table S1. Crystal data and structure refinements for **1**

1	
Formula	C ₂₇₀ H ₃₆₈ N ₂₆ O ₁₄₃ Mg ₁₆
Fw.	6654.86
Crystal system	Cubic
Space group	<i>Im-3m</i>
<i>a</i> (Å)	35.19380(10)
<i>b</i> (Å)	35.19380(10)
<i>c</i> (Å)	35.19380(10)
α (°)	90
β (°)	90
γ (°)	90
<i>V</i> (Å ³)	43591.2(2)
<i>Z</i>	6
<i>D_c</i> (g·cm ⁻³)	1.521
data collected	7.34 - 65.22
unique refl. (<i>R</i> _{int})	0.0727
GOF on <i>F</i> ²	1.010
<i>R</i> ₁ [<i>I</i> ≥ 2σ(<i>I</i>)] ^a	0.1487
<i>wR</i> ₂ [<i>I</i> ≥ 2σ(<i>I</i>)] ^b	0.2497

^a $R_I = \sum ||F_o| - |F_c|| / \sum |F_o|$. ^b $wR_2 = [\sum [w(F_o^2 - F_c^2)^2] / \sum w(F_o^2)^2]^{1/2}$, where $w = 1/[\sigma^2(F_o)^2 + (aP)^2 + bP]$ and $P = (F_o^2 + 2F_c^2)/3$.

Table S2. Selected bond lengths (\AA) and angles ($^\circ$) for **1**.

1					
Mg(1)-O(1)	2.051(4)	Mg(1)-O(3)	2.053(4)	Mg(1)-O(1W)	2.031(10)
Mg(1)-O(2W)	2.151(13)	Mg(2)-O(2)	2.233(7)	Mg(2)-O(8)	1.960(10)
Mg(2)-O(2W)	2.129(12)	Mg(2)-O(3W)	2.080(15)		
O(1)-Mg(1)-O(3)	175.93(18)	O(1)-Mg(1)-O(2W)	99.0(3)	O(3)-Mg(1)-O(2W)	84.9(3)
O(1W)-Mg(1)-O(1)	87.6(4)	O(1W)-Mg(1)-O(3)	88.6(4)	O(1W)-Mg(1)-O(2W)	170.7(7)
O(8)-Mg(2)-O(2)	96.3(3)	O(8)-Mg(2)-O(2W)	179.4(7)	O(8)-Mg(2)-O(3W)	89.0(5)
O(2W)-Mg(2)-O(2)	84.2(4)	O(3W)-Mg(2)-O(2)	174.5(6)	O(3W)-Mg(2)-O(2W)	90.5(6)
Mg(2)-O(2W)-Mg(1)	118.3(8)				

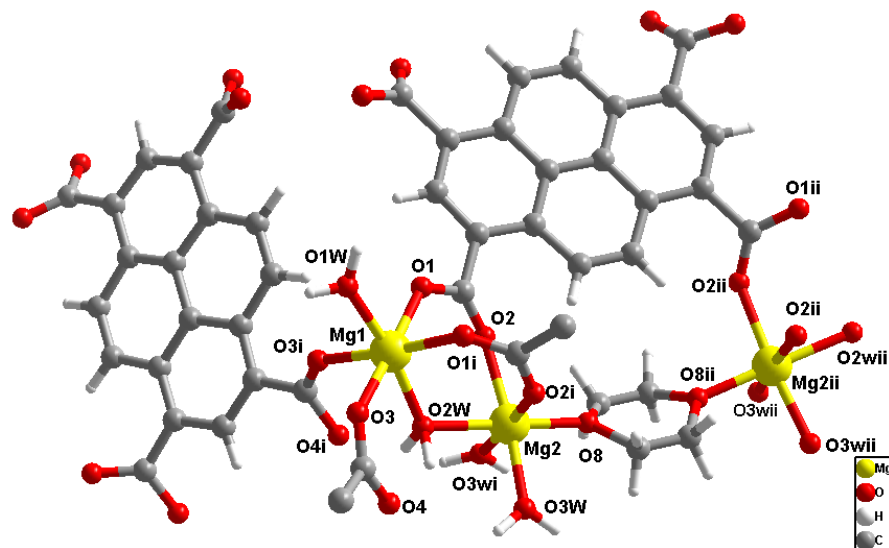


Fig. S2. The coordination environments of Mg(II) in **1** (symmetry operations: i: y, x, z; ii: y, x, -z).

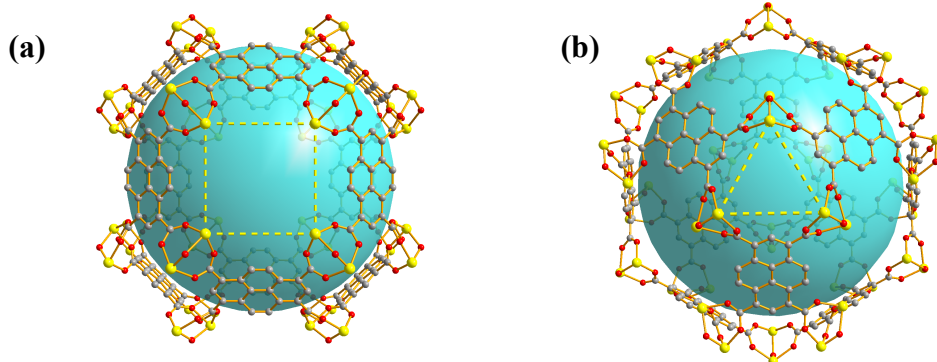


Fig. S3. Two types of windows in the cage of **1**: (a) square; (b) triangular (hydrogen atoms are omitted for clarity).

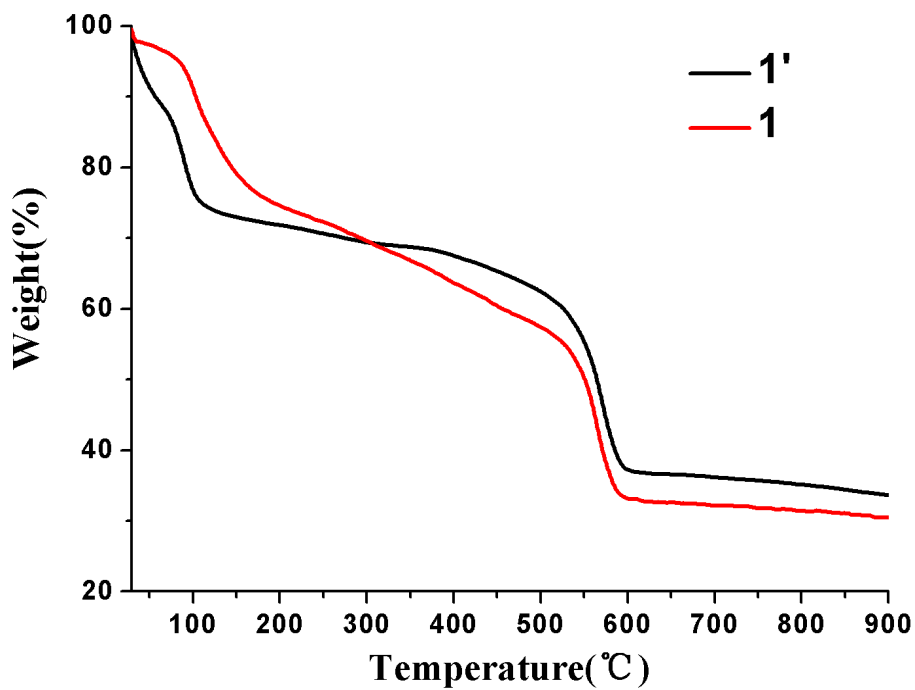


Fig. S4. TG curves for **1** and **1'**.

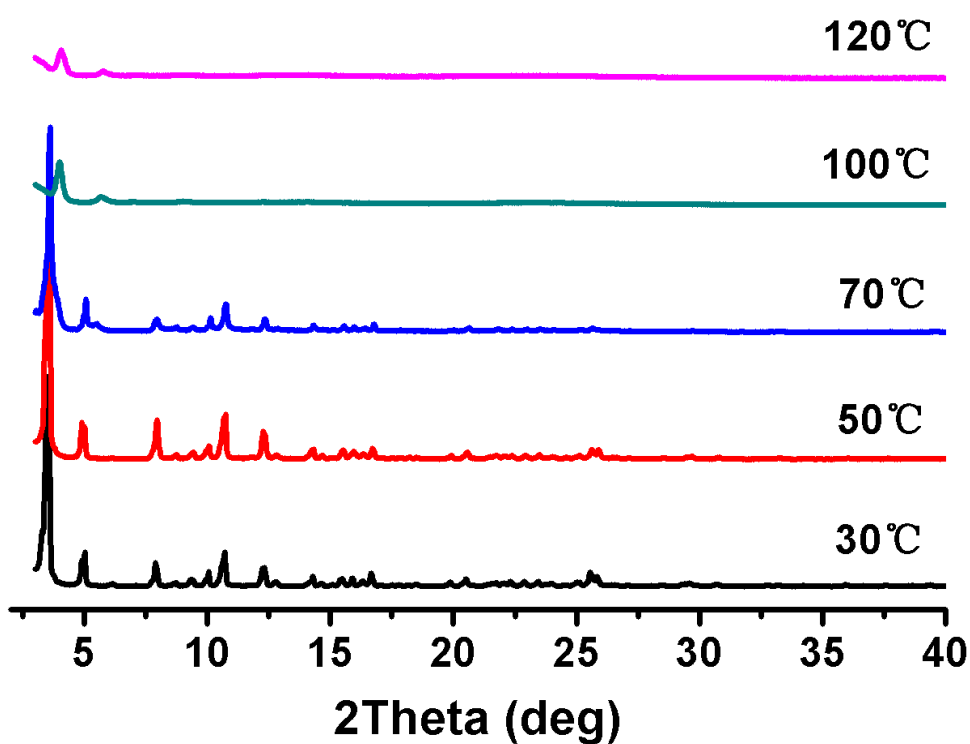


Fig. S5 The variable temperature XPRD patterns for **1'**.

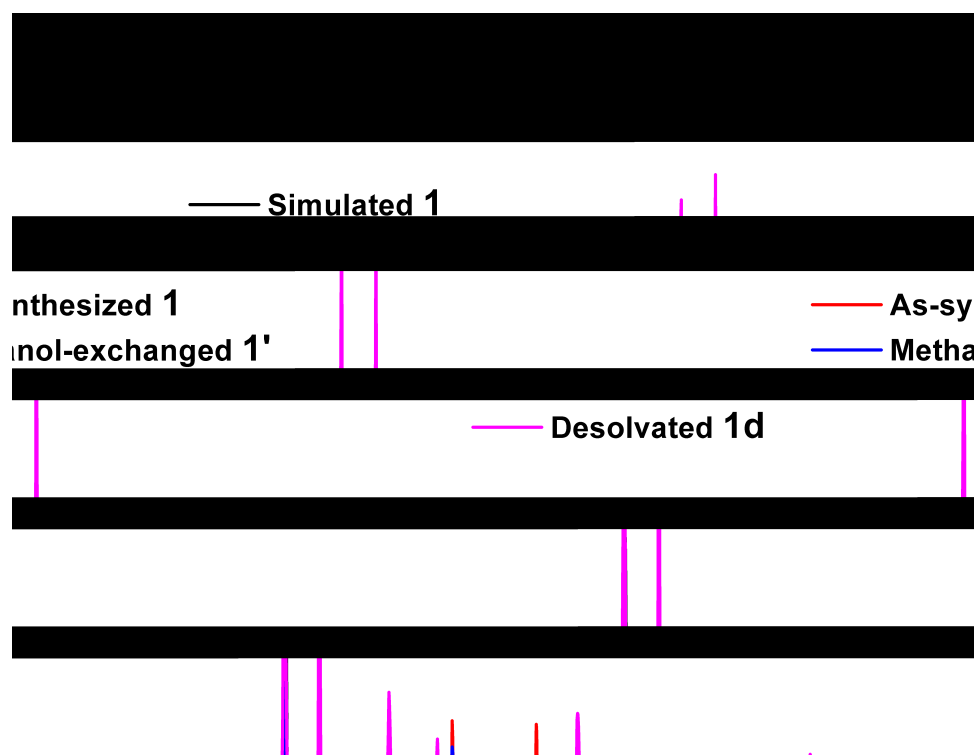


Fig. S6 The XPRD patterns for **1**, methanol-exchanged **1'** and desolvated **1d** after the gas sorption measurements.

Gas sorption measurements. Low-Pressure N₂, H₂, CO₂ and O₂ adsorption isotherms were measured with a Micromeritics ASAP2020 gas adsorption instrument. The cryogenic temperature of 77 K required for N₂, O₂ and H₂ sorption tests was controlled using liquid nitrogen bath. The cryogenic temperature of 195 K required for CO₂ sorption tests was controlled using dry ice-acetone bath. The temperatures of 273 K and 298 K required for CO₂, N₂ and O₂ sorption test was controlled using ice and water bath, respectively. The solvent-exchanged sample **1'** was prepared by immersing the as-synthesized **1** in methanol for 7 days, the extract was decanted every 12 hours and the fresh methanol was replaced. The initial outgassing process for the sample was carried out under a high vacuum (less than 10⁻⁶ mbar) at room temperature for 5 h, and the amount of weight loss (27%) is consist with that of TG analysis (28%) of **1'**, indicating all the methanol was removed from the pores. The desolvated sample and sample tube were weighed precisely and transferred to the analyzer.

Analysis of carbon dioxide adsorption.

The methods are applied to dispose the sorption data according to the literature.² The Langmuir-Freundlich equation is used to fit CO₂ adsorption isotherm and predict the adsorption capacity of the framework at saturation, and Clausius-Clapeyron equation is applied to the calculation of the enthalpies of CO₂ adsorption.

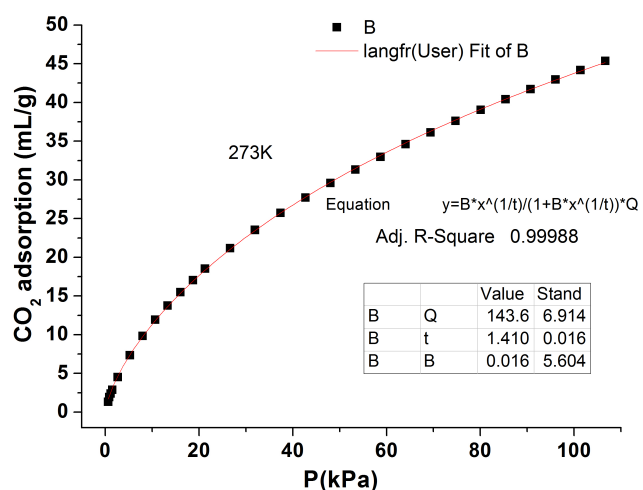


Fig. S7 Carbon dioxide isotherm at 273 K (symbols) and Langmuir-Freundlich equation fits (line) for **1d**.

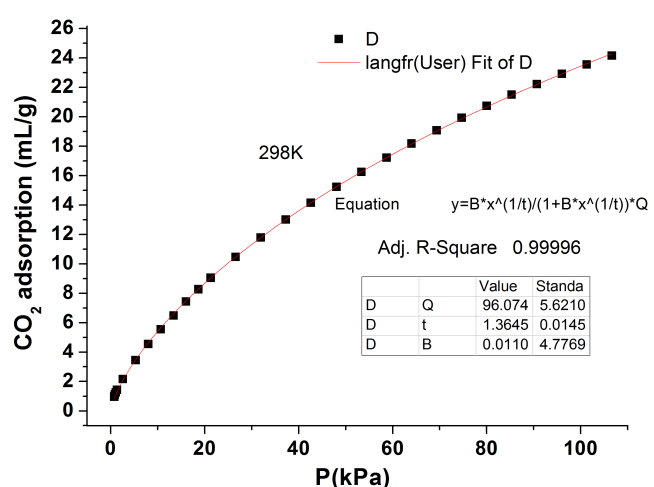


Fig. S8 Carbon dioxide isotherm at 298 K (symbols) and Langmuir-Freundlich equation fits (line) for **1d**.

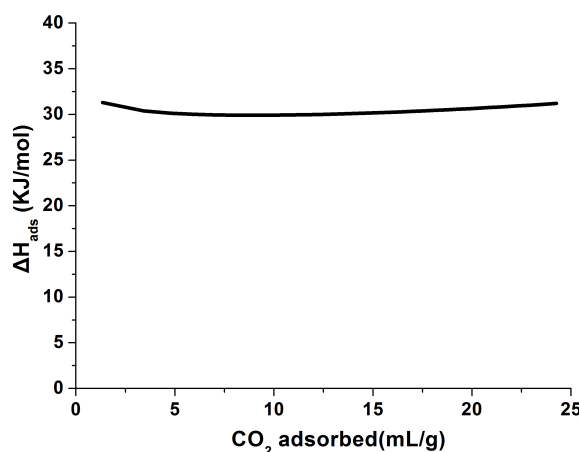


Fig. S9 The adsorption enthalpies of CO₂ calculated by Clausius-Clapeyron equation.

Calculation of CO₂/N₂ and CO₂/O₂ selectivity.

The ideal adsorbed solution theory (IAST) method used to estimate the CO₂/N₂, and CO₂/O₂ selectivity is according to the literature.³ The IAST assumes that the adsorbed phase is a two-dimensional solution in equilibrium with the bulk phase. For binary adsorption of A and B, the IAST requires:

$$yp_t = xp_a \quad (1)$$

and

$$(1 - y)p_t = (1 - x)p_b \quad (2)$$

where y and x denote the molar fraction of A in the bulk phase and the molar fraction of A in the adsorbed phase, respectively, p_t is the total gas pressure, p_a and p_b are the pressure of component a and b at the same spreading pressure as that of the mixture, respectively.

The adsorption isotherms of the pure components can be fitted by the Langmuir model:

$$q = q_t \frac{bp}{1 + bp} \quad (3)$$

Furthermore, the molar fraction of A in the adsorbed phase can be obtained from the following equation:

$$q_{t,a} \ln \left(1 + \frac{b_a p_t y}{x} \right) - q_{t,b} \ln \left(1 + \frac{b_b p_t (1-y)}{1-x} \right) = 0 \quad (4)$$

where $q_{t,a}$ and b_a are Langmuir fitting parameters of adsorption equilibrium of pure A, $q_{t,b}$ and b_b are Langmuir fitting parameters of adsorption equilibrium of pure B. The unknown x in Eq. (4) can be solved by Matlab (Version 6.0, The MathWorks, Inc.) for fixed p_t and y values.

Then calculated the predicted adsorption selectivity, which is defined as $(x_1/y_1)/(x_2/y_2)$, where x_i and y_i are the mole fractions of component i ($i = 1, 2$) in the adsorbed and bulk phases, respectively.

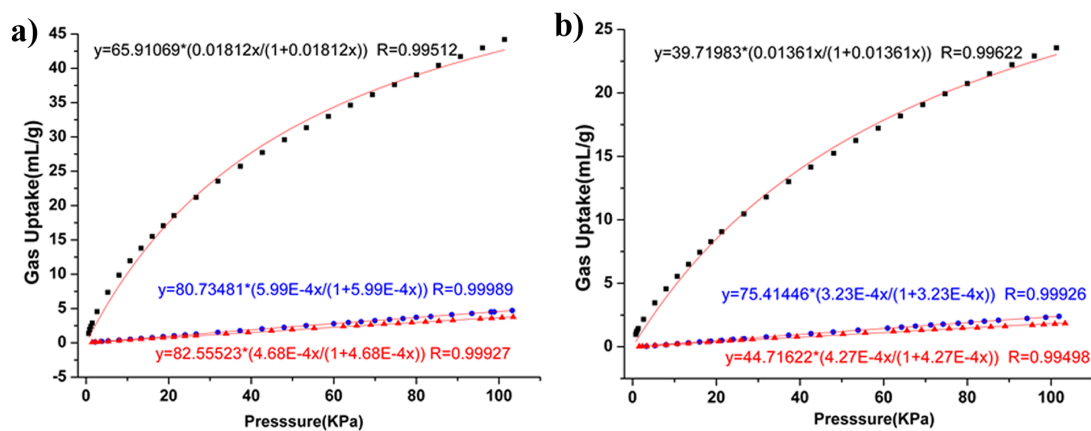


Fig. S10. The Langmuir fitting for CO₂, N₂ and O₂ isotherms a) at 273 K, and b) at 298K (CO₂: black squares; N₂: red triangles; O₂: blue circles).

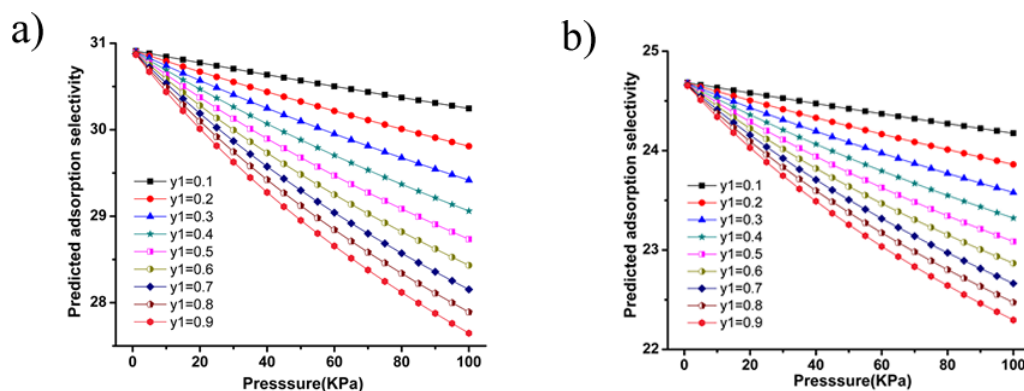


Fig. S11. Predicted adsorption selectivity of **1d** for a) CO₂ over N₂, b) CO₂ over O₂ at 273K. The y₁ denote the molar fraction of CO₂ in the bulk phase.

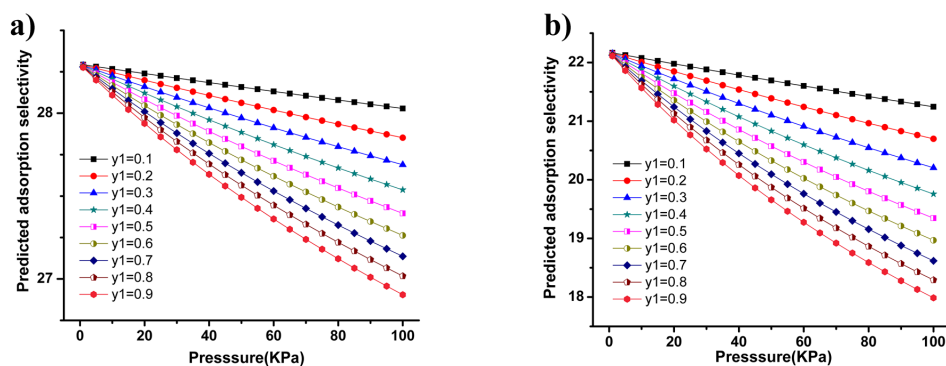


Fig. S12. Predicted adsorption selectivity of **1d** for a) CO₂ over N₂, b) CO₂ over O₂ at 298K. The y₁ denote the molar fraction of CO₂ in the bulk phase.

References

- 1 K. Ogino, S. Iwashima, H. Inokuchi and Y. Harada, *Bull. Chem. Soc. Jpn.*, 1965, **38**, 473.
- 2 M. Dincă and J. R. Long, *J. Am. Chem. Soc.*, 2005, **127**, 9376.
- 3 (a) Y. S. Bae, K. L. Mulfort, H. Frost, P. Ryan, S. Punnathanam, L. J. Broadbelt, J. T. Hupp and R. Q. Snurr, *Langmuir*, 2008, **24**, 8592; (b) J. Peng, H. Y. Ban, X. T. Zhang, L. J. Song and Z. L. Sun, *Chem. Phys. Lett.*, 2005, **401**, 94; (c) B. S. Zheng, J. F. Bai, J. G. Duan, L. Wojtas and M. J. Zaworotko, *J. Am. Chem. Soc.*, 2011, **133**, 748.